Electron Slowing-Down Spectrum in Irradiated Silicon*

L. C. Emerson, R. D. Birkhoff, V. E. Anderson, and R. H. Ritchie
Health Physics Division, Oak Ridge National Laboratory, Oak Ridge, Tennessee 37830
(Received 7 August 1972)

An electron slowing-down flux spectrum has been measured for β particles, δ rays, and secondaries in neutron-activated silicon over the energy range from a few eV to 30 keV. The spectrum is found to be similar to slowing-down spectra generated in metals by β particles. Absolute agreement with predictions of the Spencer–Fano theory is found for energies above 10 keV. Experimental fluxes are somewhat larger for lower energies. A companion theoretical calculation has been carried out based on model cross sections for Si. These include the effects of plasmon creation and electron-hole pair production in the valence band and excitation of electrons from the K and L levels. The latter processes were described on the basis of sum-rule-corrected classical cross sections. Monte Carlo calculations of the slowing-down spectrum were made. The present theory, as well as an empirically shell-corrected Spencer–Attix theory, gives spectra which are smaller than experiment by a factor of ~ 4 in the 10- to 100-eV range.

I. INTRODUCTION

When a medium is irradiated by ionizing radiation of any type a flux of electrons is generated. If the medium is essentially of infinite extent, one's attention can be focused on the generation and slowing down of these electrons without regard for geometrical or boundary effects. As the Compton electrons or photoelectrons or β rays slow down in the medium they generate other electrons. The more energetic of these are called "δ rays," whereas those of a few tens of eV or less are described generically as "secondaries." A calculation of the flux of primary electrons and δ rays was first carried out by Spencer and Fano.[1] In their theory these authors used the Møller electron-electron scattering cross section for calculating the δ-ray flux generated by the primary electrons. These δ rays when added to the primary electron give the total electron flux in the medium. The flux we shall be concerned with here is assumed to be everywhere isotropic within the medium and integrated over 4π steradians. This flux is identical with the differential track-length distribution in the medium; that is, typical units for the flux might be electrons/cm^{2}eV, and if this spectrum is normalized to one electron created per cm^3, then the units of this normalized flux spectrum are cm/eV. Thus, the flux is in fact the number of centimeters traveled by electrons as they slow down through an inifinitesimal energy interval per unit energy interval.

Some eight years ago a group at the Oak Ridge National Laboratory began attempts to measure the electron flux in various media irradiated by charged particles. For this it was necessary to design and construct an electron spectrometer of unusually large transmission and reasonably good resolution. Radioactive sources were used to ensure that the source distributions were uniform and isotropically emitting. Sources were typically two coinlike metallic discs coaxially mounted so that the space between them represented a cavity in an infinite isotropic medium. Electrons escaping from this cavity into the spectrometer were assumed to be representative of the flux in an infinite medium. The use of this instrument and the comparison with the theory of Spencer and Fano for several metallic media have been described in several publications since that time. A review of these experiments and comparison with theory have been given in a recent publication[2] of the National Academy of Sciences.

II. EXPERIMENTAL APPARATUS

The spectrometer consists of two concentric spheres between which an inverse-square electric field is maintained. Electrons, of the proper energy, which leave a source on the inner sphere are brought to a focus in an annular region at the opposite end of the spectrometer. The name of the spectrometer, the Keplertron, is derived from the Keplerian orbits followed by the electrons in the inverse-square field. The instrument was designed for a transmission of 25% and an energy resolution of 6.25%. Electrons of the appropriate energy contributing to this transmission are those emitted at all azimuths and at all emission angles between 0° and approximately 30° with respect to the tangent of the inner sphere.

Because of this high transmission it is possible to use a Faraday-cup collector and a vibrating-reed electrometer instead of the more conventional Geiger–Müller counter and scaler, thus allowing operation at electron energies far below those required to penetrate a counter window and with 100% efficiency at all energies. In addition to these advantages of high transmission and low-energy op-

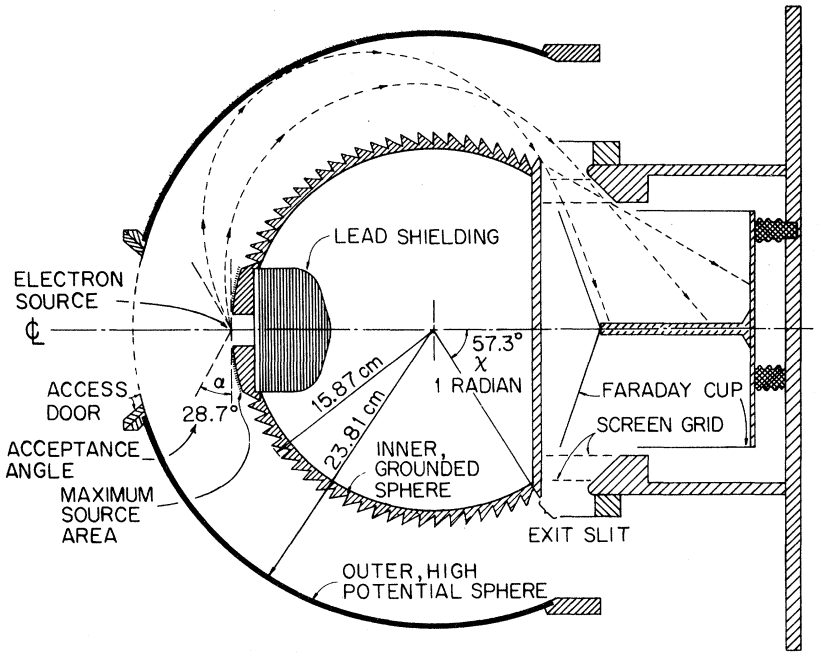

FIG. 1. The Keplertron, a high-transmission, low-energy β spectrometer.

eration, the Keplertron can be used with large sources. For instance, with the present design a source with a diameter of 3.75 in. can be used with only moderate changes in the transmission and resolution from the point-source values.

A schematic diagram of the Keplertron is shown in Fig. 1. The outer sphere consists of 0.32-cm brass rods which converge on the access door in the outer sphere across the gap from the source position. Rods were used instead of a solid sphere to minimize scattering by electrons of the wrong energy into the exit slit. The inner sphere is of solid aluminum machined with antiscatter ridges. Two grids, each made of 0.013-cm-diam gold wires, are located just inside the 2-cm-wide exit slit to reduce the capacitance between the Faraday cup and the outer sphere to 2×10^{-17} F.

Both the inner sphere and the Faraday cup are negatively biased 24 V to prevent the escape of secondary electrons produced in the cup. Additionally, both spheres and the inside of the Faraday cup are coated with acetylene soot to minimize the secondary-electron emission.

The vacuum tank containing the instrument is equipped with low-current dc coils which reduce the earth's magnetic field in the region of the Keplertron to about 30 mG. A standard liquid-nitrogen-trapped, oil-diffusion pump maintains the vacuum in the low 10^{-6}-Torr region.

In order to obtain the electron flux from measurements of the electron current it is necessary to make several corrections to the data. These are associated with the pecularities of the low-energy response of the spectrometer, its energy window, and the geometry of the source used. The corrections have been described in an earlier publication[3] and will not be repeated here.

A. Preparation of Radioactive Sources

Silicon, as it exists in nature, has three isotopes, with mass number 28 accounting for 92.18% of the normal element, mass number 29 for 4.71%, and mass number 30 for 3.12%.[4] Those isotopes with smaller mass numbers are radioactive but have half-lives which are much too short to be of any practical use to us, whereas, of the two radioisotopes with larger mass numbers, only ^{31}Si can be produced in quantities sufficient for experimental studies of the slowing-down spectrum. ^{31}Si, with a 2.62-h halflife, is most conveniently produced by an (n,γ) reaction. The activation cross section for 2200 m/sec neutrons is 110 ± 10 mb.[5] This isotope is almost a pure β emitter with only 0.07% of the disintegrations being accompanied by photon emission.[6] The decay scheme is shown in Fig. 2.

Five single-crystal silicon disks were obtained from the Instrumentation and Controls Division of

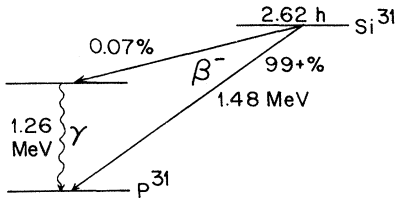

FIG. 2. Decay scheme of ^{31}Si.

the Oak Ridge National Laboratory. The disks were in the form of right circular cylinders 0.370 in. diameter, 0.102 in. thick, and weighed approximately 400 mg. These were essentially intrinsic silicon with impurity levels not exceeding several parts per billion.[7]

Prior to the initial irradiation the crystals were etched using a mixture of nitric and hydrofluoric acids. This process removed a few milligrams of silicon from the surfaces of the discs and left the faces with a clean and bright mirrorlike appearance. Just before each subsequent irradiation the crystals were washed in nitric acid followed by hydrofluoric acid. Each such cycle removes only a few atomic layers from the crystal as well as any surface contamination which may have been introduced in handling.

Following the cleaning process the crystals were mounted in the irradiation capsules using sterile techniques. The presence of any foreign material on the surfaces of the crystals can lead to impurity activities which may distort the measured spectrum as well as change the work function of the crystal and mechanically impede the escape of the low-energy electrons.

The neutron irradiations were carried out in both the Oak Ridge Research Reactor at a thermal flux of approximately 2×10^{14} $n/\mathrm{cm}^2\,\mathrm{sec}$ and the High Flux Isotope Reactor at 2.9×10^{15} $n/\mathrm{cm}^2\,\mathrm{sec}$. The irradiation obtained using the higher flux produced a source strength of 4.4×10^{11} disintegrations/sec cm^3. The final analysis was made using data obtained with this source because of the generally better statistics.

The source strength used in the analysis was calculated using the known neutron flux, the isotopic abundance of ^{30}Si, and its activation cross section. An independent check of the source strength was obtained by a photon count of the 1.26-MeV photopeak using a sodium iodide crystal and multichannel analyzer previously calibrated with the 1.27-MeV photon from a ^{22}Na standard obtained from the National Bureau of Standards.

The measured photon spectrum is shown in Fig. 3. The steep continuum at lower energies is characteristic of the bremmstrahlung from the absorption of the β particles in the aluminum shield between the disc and the NaI crystal. The two peaks at 0.420 and 0.516 MeV, as well as the slight shoulder on the high-energy side of the silicon photopeak, are contaminating activities which were probably introduced by exposure to the hot-cell environment during transfer of the source from the irradiation cell to the Keplertron holder.

B. Electron Slowing-Down Spectrum

In Fig. 4 we have plotted the electron slowing-down spectrum for the silicon β rays in silicon. Three estimates of the flux are shown: the theoretical curve of Spencer and Fano as obtained by interpolation in the tables of McGinnies,[1] the flux outside the surface barrier of the silicon as indicated by the solid dots, and the flux inside as inferred from the outside measurements using a suitable barrier-penetration factor. Because of the roughness of the emitting surfaces, we have chosen to integrate the classical probability for transmission of an electron incident at a certain angle on a potential barrier over all angles of incidence. The over-all transmission for an isotropically incident flux for an electron of energy E is then

$$T=1-\left(\frac{\phi-E_g}{E+\phi-E_g}\right)^{1/2},$$

where ϕ is the work function and E_g is the energy gap. The zero of energy is the bottom of the conduction band for the flux inside the medium and the vacuum level for the flux outside. The Spencer–Fano theory is relatively independent of the slowing-down medium—metal, semiconductor, insulator—inasmuch as it relies upon the Møller free-electron scattering cross section for production of δ rays. The theoretical curve shows a high-energy part (above 10^4 eV), wherein the spectral shape is dominated by the primary β rays in a very simple manner. In the continuous-slowing-down approximation used by Spencer and Fano the flux is given basically by the ratio of the number of electrons created above a given energy to the stopping power at that energy. Since the stopping power is relatively constant above a few tens of keV, the theory is essentially the integral primary nuclear β-ray spectrum. At about 10^4 eV the number of δ rays is comparable with the number of primaries, and below this energy the further generations of δ rays dominate the theoretical spectrum. Unfortunately, the theory describes only δ rays rather than the low-energy secondaries and hence is not applicable below about 500 eV. The experimental data indicate that the flux increases more rapidly than the theory predicts as the energy is reduced, acquiring a roughly $1/E$ behavior between about 20 keV and 20 eV, with a somewhat larger energy dependence below this energy. This behavior is similar to that which has been noted previously for metallic slowing-down media. Some evidence of the structure is seen in the data at about 1.8 keV and 100 eV, the K- and L-shell binding energies in silicon. The flux immediately above these energies is depleted by virtue of electrons which ionize the shells, losing an amount of energy at least equal to the shell energy and thus skipping over the energy interval above the shell energy. A further reduction occurs because the stopping power is greater just above the shell energy. Shell ionization is followed by Auger emission which

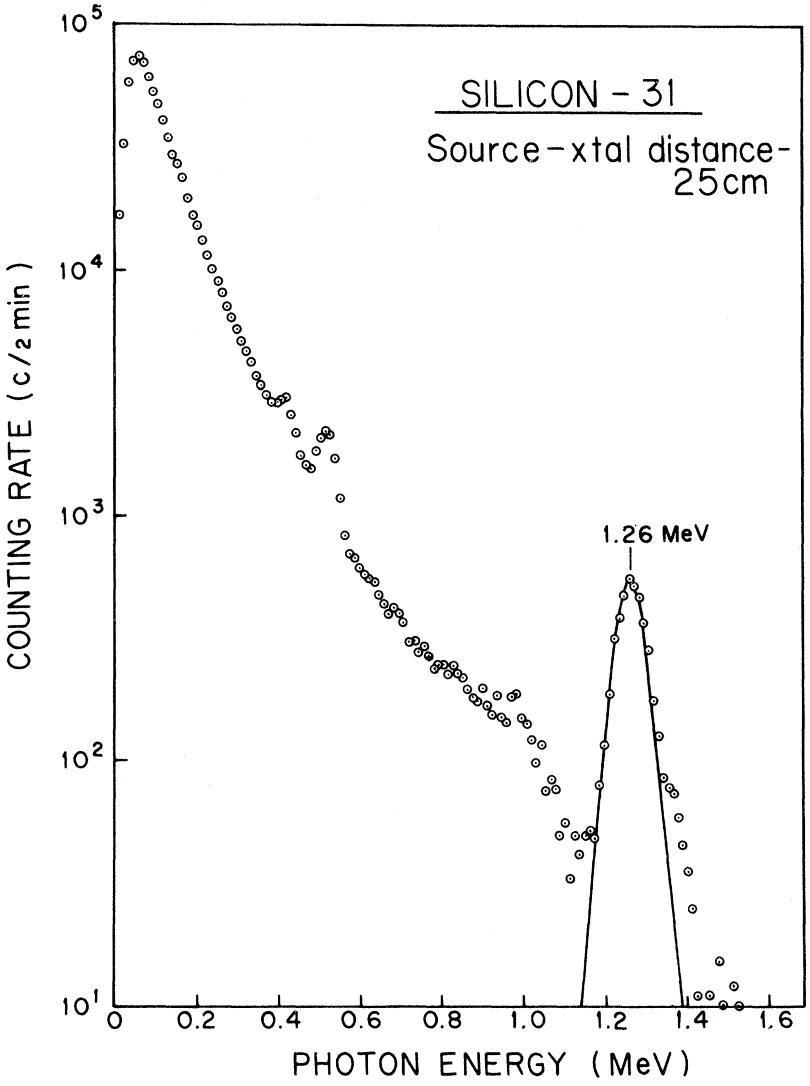

FIG. 3. γ-ray spectrum of typical silicon source.

constitutes a new source of electrons in the medium. This, coupled with the reduced stopping power below the shell energy, increases the flux. Thus the four effects combine to cause a discontinuity in the data ranging up to 60% for some sources. The heights of the discontinuities were found to depend rather importantly on the state of the surface of the emitting discs. This is the first time such shell effects have been observed in non-K-capture isotopes and represent a breakdown in the continuous-slowing-down model.

To summarize, the electron flux in β-irradiated silicon has been measured over the energy range from a few eV to 30 keV. The spectrum is found to be similar to that in metals irradiated similarly and, while agreeing with the Spencer–Fano theory on an absolute basis above 10 keV, indicates a somewhat larger electron flux at lower energies. Spectra such as these are useful in calculation of radiation-induced effects in media. That is, the product of the cross section for any event and the flux, when integrated over the energies in the flux, gives the yield for this particular event. Calculations of this sort have been reported recently by some of us.[8]

III. THEORY

In a theoretical effort paralleling the experimental study described above, calculations of electron slowing down in a model semiconductor have been made. Progress in this effort requires detailed estimates of differential inelastic cross sections for excitation of valence-band and inner-level electron transitions for incident energies ranging from a few eV to 10^6 eV.

Spencer and Fano[1] and Spencer and Attix[9] have given a theoretical treatment of electron slowing-down spectra at energies high enough that detailed

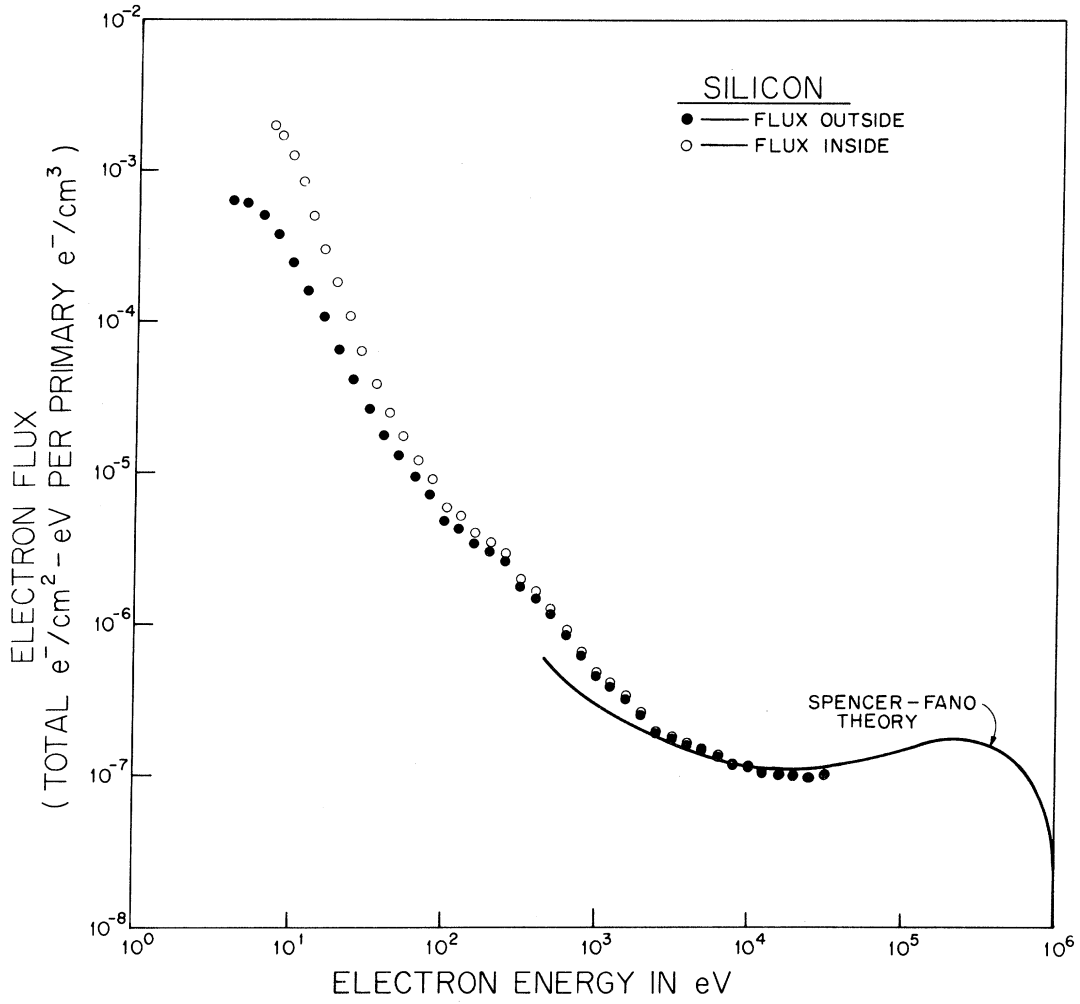

FIG. 4. Measured electron slowing-down cascade in silicon.

electronic structure of the material is not important. Calculations at energies comparable with transition energies from inner levels require not only detailed cross sections which account for binding effects but also require a different approach to the solution of the Boltzmann equation. The Spencer–Fano method is predicated upon the approximate validity of the continuous-slowing-down approximation (CSDA); this approximation is suspect in this range of energies where the probability of large fractional energy losses becomes appreciable. Recently, Klots and Wright[10] and Sherman and Gordon[11] have employed various schematic cross sections to solve for the slowing-down spectrum in model systems, using methods not based on the CSDA.

The work reported here has involved the use of (a) the Callaway–Tosatti[12,13] model of a semiconductor to generate cross sections for excitation from the valence band, (b) classical cross sections[14–16] for excitations from inner levels, and (c) the Kane[17] cross sections for electron interaction with the phonon field. These cross sections have been prepared for use in a Monte Carlo code which was designed and written by some of us for another application.[18,19] This code has been used to compute slowing-down spectra in Si. Comparisons with experimental data and with calculations based on the Spencer–Attix model have been made and are discussed below.

A. Cross Sections

There is little theoretical or experimental information about electron inelastic cross sections in semiconductors over the range of energies covered in our experiment. Kane[17] has computed the mean free path of electrons of a few eV energy against electron-hole pair creation in crystalline silicon. He also calculated the mean free path against phonon scattering in the same energy range. Experi-

mental data on photoemission and electron emission from a reversed-bias p-n junction tend to confirm his results to within a factor of 2; some uncertainty attends the process of inferring mean free paths from these data. In the high-energy region (> 10 keV) the Bethe theory[20] may be used to compute electron stopping power in Si accurate to a few percent. Differential cross sections are not predictable to such accuracy on a quantum mechanical perturbation-theoretic basis since reliable wave functions for excited states in the solid are not available.

In lieu of definitive data, estimates of relevant differential inelastic cross sections must be made. Two different models have been used for this purpose.

1. *Valence-Band Excitation*

The Callaway–Tosatti[12,13] model of a semiconductor possesses the advantage of simplicity and analytical convenience. It can provide detailed estimates of the dynamical response characteristics of such materials. Penn[21] has proposed a more complete model of a crystalline semiconductor which provides for the possibility of umklapp scattering processes on the lattice. The dielectric response function in this model has been studied by Brandt and Reinheimer.[22] The single-crystal silicon used in the present experiment must experience considerable radiation damage during exposure, leading to appreciable disruption of its structure. Brandt and Reinheimer[23] have suggested that the response function of an amorphous semiconductor may be approximated by neglecting umklapp processes which are important for crystalline material. Hence we have employed the Callaway–Tosatti model to estimate cross sections for valence-electron excitation in our silicon samples.

In this model the dielectric response function $\epsilon(k, \omega) = \epsilon_1 + i\epsilon_2$ of a semiconductor is derived in the random-phase approximation. Following Tosatti,[13] a single isotropic energy gap is introduced into an electron gas; the sum rule requirement

$$\int_0^\infty \omega\epsilon_2(k, \omega)\, d\omega = 2\pi^2 ne^2/m^*$$

is imposed. Here n is the valence-band electron density and m^* is the effective mass of the electron. The dynamical response function depends parametrically upon n and g, the energy gap in units of the Fermi energy. Expressions for ϵ_1 and ϵ_2 valid over the whole of the (k, ω) plane have been derived on this basis and are given in the Appendix. The theory of electron response in this model semiconductor is fairly intricate. Here we deal in detail primarily with the total inverse mean free path. A fuller description will be given elsewhere.

Figure 5 shows $a_0\Sigma_e(E)$ and $a_0\Sigma_p(E)$ where Σ_e is the inverse mean free path for electron-hole pair excitation by an electron of energy E and $\Sigma_p(E)$ is the inverse mean free path for plasmon creation. Both quantities are plotted as a function of energy measured from the bottom of the band gap and in units of E_F, the Fermi energy in the model. a_0 is the first Bohr radius ($a_0 = \hbar^2/me^2 = 0.529$ Å).

The expression used in obtaining our numerical results for $\Sigma_e(E)$ is

$$\Sigma_e(E) = [a_0\pi(E+1)]^{-1} \int_0^{E-g} dx \int_{z_{\min}}^{[(1+x-g)^{1/2}+1]/2} dz \; \frac{\chi^2 f_2(x, z)}{[z^2 + \chi^2 f_1]^2 + [\chi^2 f_2]^2} \,, \tag{1}$$

representing integrations over energy and momentum transfer variables consistent with the energy-momentum dispersion property of the electron. The quantities f_1 and f_2 are defined in terms of the complex dielectric constant $\epsilon(x, z)$ as follows:

$$\epsilon(x, z) = 1 + (\chi^2/z^2)\,[f_1(x, z) + if_2(x, z)] \,, \tag{2}$$

where x is the energy transferred to the electronic system in units of E_F, z is the momentum transferred to the system in units of $2k_F\hbar$, $\chi^2 = (\mathcal{R}/\pi^2 E_F)^{1/2}$, $\mathcal{R} = e^2/2a_0$, and $k_F = (2mE_F)^{1/2}/\hbar$. The lower limit on the z integration above, $z_{\min}$, is defined as the smaller of the two quantities $\frac{1}{2}[(1+x-g)^{1/2} - 1]$ and $\frac{1}{2}[(1+E)^{1/2} - (1+E-x)^{1/2}]$.

The magnitude of energy gap in our model semiconductor has been adjusted so that $\Sigma_e(E)$ gives reasonable agreement with Kane's calculations and with an experimental value[17] of $\Sigma_e(E)$ at 5 eV. This choice was $g = 0.14$, while E_F was taken to be 12.78 eV. The experimental value is shown as the open circle, while Kane's theoretical values are shown as filled-in circles on this curve. Kane has carried out random-phase-approximation (RPA) calculations of the electron mean free path in Si on the basis of band-structure theoretic work done by him; unfortunately, this was done over a rather limited range of energies. We have fitted the experiment and theory in an average way since uncertainties attend both kinds of data.

In Fig. 6 we display a graph of the quantity $a_0(1+E)\,d\Sigma_e/dx$ vs x as calculated for a fast electron with energy $E > 1$ (Energy $> E_F$). In this graph x is the energy lost by the fast electron in electron-hole pair creation, and $d\Sigma_e/dx$ is the differential probabil-

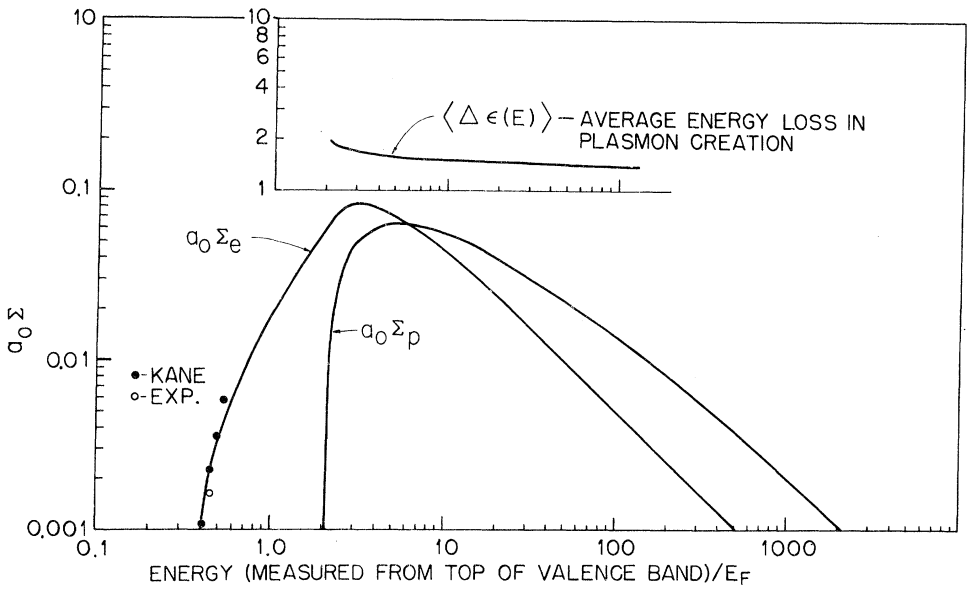

FIG. 5. Inverse mean free path for valence-band excitation in Si as a function of electron energy measured from the top of the valence band and in units of the Fermi energy. Σ_e is the inverse mean free path for electron-hole pair creation and Σ_p is that for plasmon creation. Also shown in the same energy scale is $\langle \Delta\epsilon(E) \rangle$, the mean energy lost in plasmon creation as a function of E.

ity per unit length for that process. The parameter g was taken to be 0.3 for this calculation. It may be noted that this distribution rises to a maximum value at an energy loss somewhat greater than the plasma energy and descends monotonically as energy increases to still larger values, approaching asymptotically the function const$\times x^{-2}$, characteristic of transfer to an ensemble of free electrons.

The inverse mean free path for plasmon creation was computed from

$$\Sigma_p(E) = [a_0(E+1)]^{-1} \int_0^{E-g} \frac{z_0(x)\,dx}{|2z_0(x) + \chi^2 df_1(x, z_0(x))/dz|}, \tag{3}$$

where $z_0(x)$ is the equation of the plasmon dispersion line. Figure 7 shows a plot of the inverse relation $x = x_0(z)$ for the plasmon in Si as computed from the present model. In Fig. 5 we also display $\langle \Delta\epsilon(E) \rangle$, the mean energy lost by an electron of energy E in creating a plasmon.

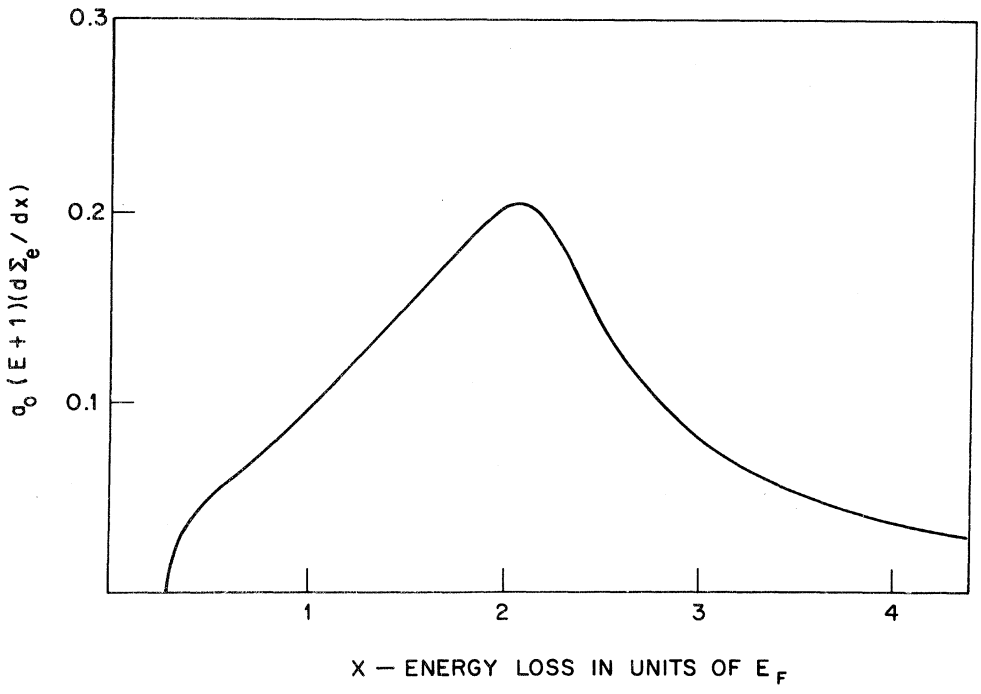

FIG. 6. The differential inverse mean free path for loss of energy x by a fast electron of energy E in creating an electron-hole pair in a model semiconductor. All energies are measured from the top of the valence band and in units of E_F. The energy gap was taken to be 0.3 E_F to obtain these results.

2. Excitation from Deep-Lying Levels

Estimates of cross sections for excitation from inner levels in solids are rather uncertain, particularly in the neighborhood of the thresholds. Wave functions for inner levels are likely to be similar to those of the corresponding isolated atom. There is expected to be an energy shift from free-atom values of magnitude small compared with binding energies for deeper levels. However, widths of the energy bands corresponding to inner levels may be quite narrow. By contrast, the unfilled levels of the condensed matter are changed considerably. The discrete spectrum of the isolated atom is missing, and there remains a series of bands which merge into a free-electron continuum for high enough energies. The energy gap for valence-band excitation is quite small compared with excitation energies from inner levels. To simplify matters and to obtain convenient analytical formulas which have acceptable behavior overall, classical "impulse" or binary collision cross sections for inner-level excitation have been employed in the work described here.

The present approach to this problem consists of employing sum-rule-corrected classical (binary collision) cross sections to represent excitation from the various inner levels. Excitation energies of each level may be adjusted to agree with experimental data, while the generalized oscillator strengths corresponding to the several transitions may be adjusted to yield the correct total high-energy stopping power. Atomiclike (hydrogenic) speed distributions of electrons in the ground states of the various levels have been employed.

The differential inverse mean free path $d^2\Sigma_i/d\epsilon\, d\eta$ for excitation of the ith inner level may be written[15,24] in the present approximation as

$$\frac{d^2\Sigma_i(\epsilon,\eta)}{d\epsilon d\eta} = \frac{A_i}{a_0\xi\eta\epsilon}\,\frac{d}{d\epsilon}\,f_i(\epsilon,\eta)\,. \tag{4}$$

Here $df_i/d\epsilon$ is the generalized differential oscillator strength for transitions from the ith level in which energy $E_i\epsilon$ and momentum $(2mE_i)^{1/2}\eta$ are

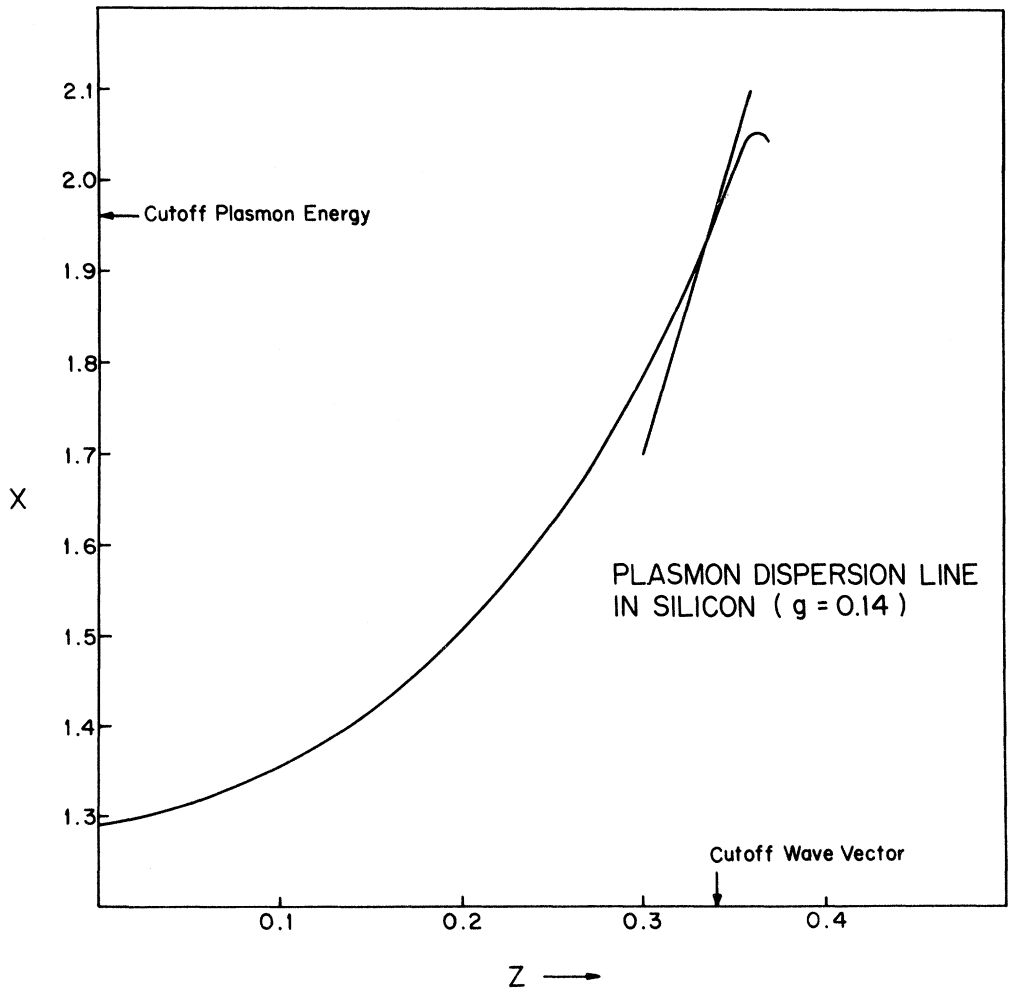

FIG. 7. The plasmon dispersion relation for a model semiconductor. This curve relates the eigenenergy $E_F x_0(z)$ of the plasmon with the momentum $2\hbar k_F z$ carried by the plasmon.

transferred to the excited electron. E_i is the mean kinetic energy of an electron in the ground state of the ith level. The energy of the primary electron is $E_i\xi$. The constant $A_i = 8\pi a_0^3 N_i (\mathcal{R}/E_i)^2$, where $a_0 = \hbar^2/me^2 = 0.529$ Å, $\mathcal{R} = e^2/2a_0 = 13.6$ eV is the Rydberg energy, and N_i is the total number of electrons in the ith level per unit volume of the material. The generalized differential oscillator strength is assumed to satisfy the sum rule

$$\int_{\epsilon_{0i}}^{\infty} \frac{df_i(\eta, \epsilon)}{d\epsilon}\, d\epsilon = 1$$

in the present model. The smallest energy required to excite an electron from the ith level is equal to $\epsilon_{0i} E_i$. Clearly only those values of η and ϵ which are consistent with energy-momentum conservation by the fast electron should be considered in Eq. (4). Thus, only that part of the η-ϵ plane lying under the parabola $\epsilon = \eta(2\sqrt{\xi} - \eta)$ and lying above the line $\epsilon = \epsilon_{0i}$ should be included in integrating the doubly differential inverse mean free path $d^2\Sigma_i/d\epsilon\, d\eta$ to obtain the total inverse mean free path. This analytic form for the maximum energy transfer follows from the assumption that the energy-momentum relation for the fast electron is parabolic when measured from the Fermi level. This assumption should lead to little error for deep-lying levels.

For the present purposes we assume that the speed distribution of electrons in the ith shell has the form $f(v) = (32/\pi)\, v^2 v_i^5 (v^2 + v_i)^{-4}$, where $v_i = (2E_i/m)^{1/2}$. This is the exact quantum distribution for a filled shell of any principal quantum number in a hydrogenic atom[25] and leads to a total cross section for the H atom which agrees surprisingly well with the quantal Born approximation at primary electron energies, even in the neighborhood of the threshold.[15] It has also been used to obtain differential cross sections for ionization of multishell atoms with results comparable with those found from the Born approximation and from experiment.[26] In the classical binary-collision model this speed distribution yields very convenient analytical results for the differential inverse mean free path for electron excitation of the ith level. It is found that

$$\frac{df_i}{d\epsilon} = \frac{2^8}{3\pi} \frac{\epsilon\eta^3}{[(\epsilon - \eta)^2 + 4\eta^2]^3} \tag{5}$$

for this case. Also,

$$\frac{d}{d\epsilon}\Sigma_i = \frac{A_i}{3\pi a_0} \frac{\vartheta(\epsilon - \epsilon_{0i})}{\xi\epsilon^3} \left[(3\epsilon + 4)\left(\tan^{-1} y + \frac{y}{1+y^2} \right) + \frac{2y(\epsilon - 4)}{(1+y^2)^2} \right], \tag{6}$$

where $y = (\xi - \epsilon)^{1/2}$ and $\vartheta(x)$ is the unit step function. In the present application we assume that accessible final states corresponding to energy transfers greater than ϵ_0 are continuously distributed in energy.

Equation (6) should give a reasonable representation of $d\Sigma_i/d\epsilon$ unless $E \gg E_i$ and $\epsilon \sim \epsilon_{0i}$. In such case there may be an appreciable contribution to $d\Sigma_i/d\epsilon$ from the range $\eta \ll 1$, in which the sum rule

$$\int_{\epsilon_{0i}}^{\infty} \frac{df_i}{d\epsilon}\, d\epsilon = 1$$

is not well satisfied. It is straightforward to show that if

$$f_i \equiv \int_{\epsilon_{0i}}^{\infty} \frac{df_i}{d\epsilon}\, d\epsilon ,$$

then from Eq. (6)

$$f_i = \frac{16\eta^3}{3\pi} \left[\frac{4 - \epsilon_{0i} + \eta^2}{D^2} + \frac{3}{32\eta^3} \left(\pi - 2\tan^{-1} \frac{\epsilon_{0i} \eta^2}{2\eta} \right) - \frac{3(\epsilon_{0i} - \eta^2)}{8\eta^2 D} \right], \tag{7}$$

where $D = (\epsilon_{0i} - \eta^2)^2 + 4\eta^2$. As $\eta \to \infty$, $f_i \to 1$ as it should. However, as $\eta \to 0$, $f_i \to 64\eta^3/3\pi\epsilon_{0i}^4$. This deficiency in oscillator strength is responsible for the often noted failure of the classical inelastic cross section to attain the correct asymptotic form $\Sigma_i(\xi) \sim (\ln\xi + \text{const})/\xi$ as ξ becomes very large. To remedy this deficiency in an approximate way we may add oscillator strength at energy losses around $\epsilon_{\xi i}$ with η-dependent amplitude $1 - f_i(\eta)$ and adjust $\epsilon_{\xi i}$ for each level so that the total stopping power including that of the valence band agrees with experiment. More accurate corrections may be made by using higher-order sum rules[20,27]; however, we feel that this prescription should be sufficiently accurate for the present purposes.

In Fig. 8 there are plotted graphs of the functions $Q(\xi)$ and $S(\xi)$ over the interval $1 < \xi < 10^3$. The function Q is related to the total inverse mean free path of a fast electron with energy ξE_i, i.e.,

$$\Sigma_i(\xi) = \int_{\epsilon_{0i}}^{\xi} d\epsilon\, \frac{d\Sigma_i}{d\epsilon} \equiv \frac{1}{2a_0} A_i\, Q(\xi) .$$

The stopping power (energy lost per unit path length) of the fast electron is related to the function $S(\xi)$ as follows:

$$-\frac{dE}{dR} = \int_{\epsilon_{0i}}^{\xi} \epsilon\, \frac{d\Sigma_i}{d\epsilon}\, d\epsilon \equiv \frac{1}{2a_0} A_i\, S(\xi) .$$

Both $Q(\xi)$ and $S(\xi)$ have been evaluated in Fig. 8, choosing $\epsilon_0 = 1$ and using the expression given in Eq. (6) for $d\Sigma_i/d\epsilon$. The requisite integrations were done numerically. The sum-rule-corrected contributions to $\Sigma_i(\xi)$ and $(-dE/dR)_i$ may be obtained directly from a function $G(x)$, where

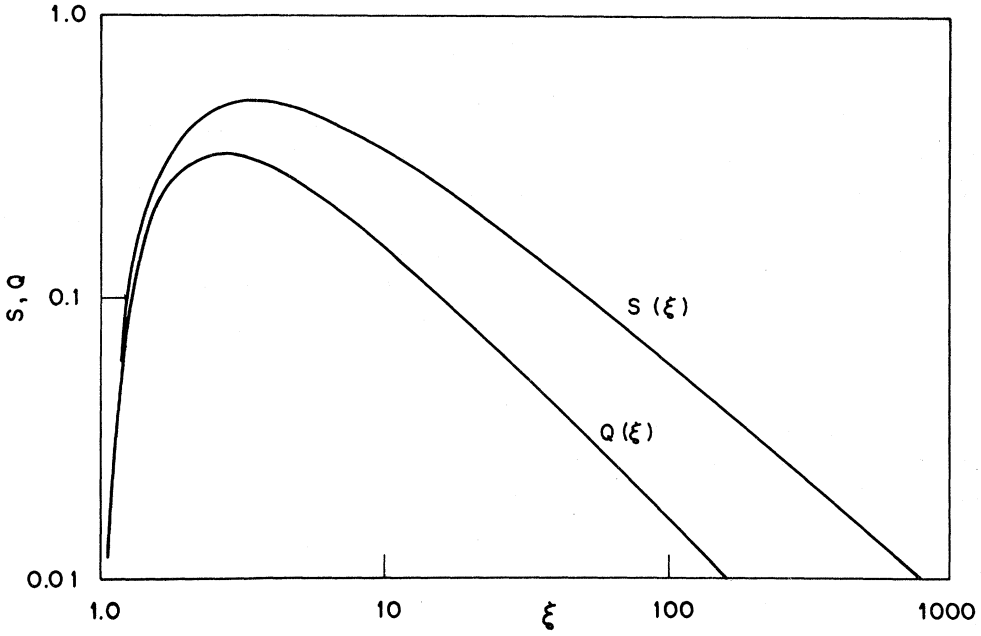

FIG. 8. Functions related to inverse mean free path and stopping power for a given energy level. The dimensionless variable $\xi = E/E_i$, where E is the energy of a fast electron and E_i is the average kinetic energy of electrons bound in the ith level. $Q(\xi)$ and $S(\xi)$ are related to inverse mean free path and stopping power, respectively, in the text.

$$G(x) = \int_x^\infty \frac{dy}{y} [1 - f_i(y)] .$$

More specifically,

$$\Sigma_i^{\text{corr}} = (A_i / a_0 \xi \epsilon_{\xi i}) G[\xi^{1/2} - (\xi - \epsilon_{\xi i})^{1/2}]$$

and

$$\left(\frac{-dE}{dR}\right)_i^{\text{corr}} = \frac{A_i}{a_0 \xi} G[\xi^{1/2} - (\xi - \epsilon_{\xi i})^{1/2}] .$$

3. *Partial and Total Stopping Power*

Figure 9 shows the total stopping power computed for all levels in silicon by the methods described above. Individual contributions from each

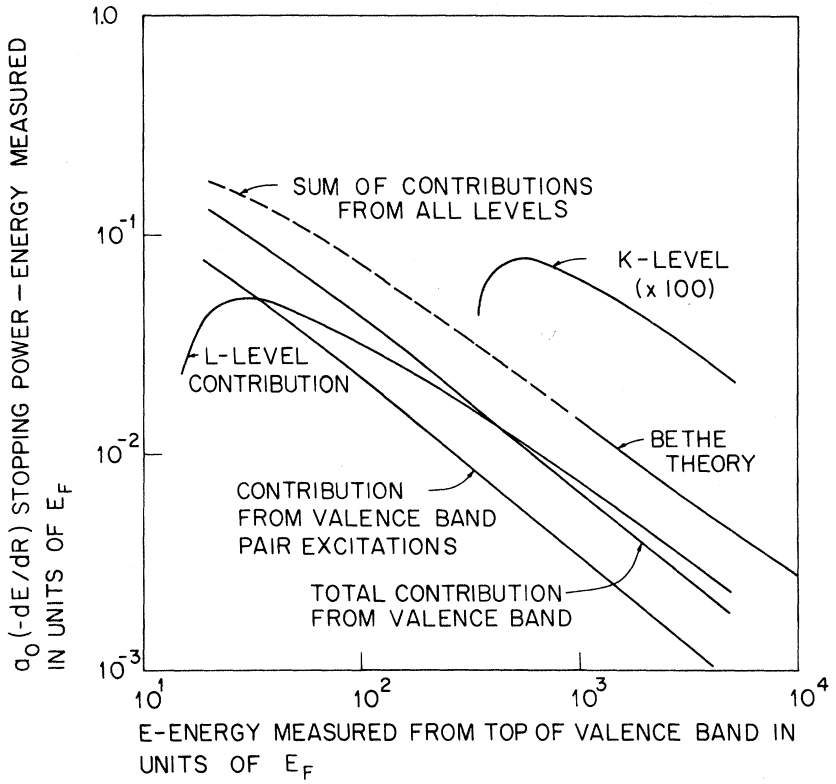

FIG. 9. Stopping power (multiplied by a_0) vs electron energy for Si. All energies are measured in units of E_F. Contributions from the K level, the L level, the total valence-band contribution, and that part of the valence-band contribution from electron-hole pair excitations are shown separately. The sum of contributions from all electrons calculated from this model is shown as a dotted line which joins smoothly with the Bethe formula at higher energies.

level and the valence band are indicated. Also shown is the high-energy Bethe stopping power computed from the nonrelativistic formula[20]

$$-\left(\frac{dE}{dR}\right)_{\text{Bethe}} = \frac{4\pi e^4 N}{mv^2} \ln\left(\frac{E}{I}\sqrt{\tfrac{1}{2}e}\right), \quad (8)$$

where N is the total density of electrons in the solid and $I = Z(9.76 + 59.8\,Z^{-1.19})$ is the adjusted mean excitation energy of an atom with atomic number Z. Using $Z = 14$, atomic weight = 28.086, density = 2.42 g/cm^3 for Si, we find

$$-\left(\frac{dE}{dR}\right)_{\text{Bethe}} = \frac{3.068}{a_0 E} \ln\left(\frac{E}{11.55}\right), \quad (9)$$

where energy is measured in units of $E_F = 12.78$ eV, the value assumed throughout our calculations.

The contribution to $(-dE/dR)$ from the L level was adjusted slightly as described above to give agreement with the Bethe form for energies above 10 keV. The K-level contribution was not adjusted since it is quite small by comparison with contributions from the L level and the valence band.

4. *Scattering of Electrons by the Phonon Field*

Kane[17] has computed the phonon scattering rate of electrons in the range 1–6 eV relative to the valence-band maximum energy. His results were adjusted to agree with an experimental value of electron-phonon mean free path ($l_{e\text{-ph}} = 60$ Å at 5 eV) from the work of Bartelink, Moll, and Meyer.[28] Kane's data were converted to mean free path as a function of energy by using his computed group velocities. The results show rather strong fluctuations in mean free path in this energy range. For higher energies the analytical form $a_0 \Sigma_{e\text{-ph}} = 0.0117/(1+E)$ was employed to represent the electron-phonon inverse mean free path. This expression gives a smoothed representation of the low-energy data and extrapolates to high energies in a reasonable way. The energy loss experienced by an electron in creating a phonon was taken to be 0.05 eV.[17]

5. *Electrons Resulting from the Filling of Holes*

As a fast electron slows down in any solid, numerous vacancies may be formed in occupied energy bands. These holes are filled subsequently by transitions of electrons from higher energy bands. The energy made available in these transitions may appear in the form of Auger-electron kinetic energy or in the form of electromagnetic field energy. Since silicon has a relatively low atomic number, Auger processes are expected to be more important than radiative processes. A hole formed on the K level of Si may be filled-in transitions from any of the L levels or from the valence band. Experimental indications[21] are that the most important transitions are from levels immediately above those in which holes exist. In general, Auger cascading of such holes may occur,[29] leading to a high degree of ionization in higher-Z materials following single ionization of K levels. Accordingly, we have allowed for Auger deexcitation of L level vacancies in Si by causing an electron to be created with energy distributed uniformly between the energies $\bar{E}_L$ and $\bar{E}_L - E_F$, where $\bar{E}_L$ is the L-level excitation energy averaged over all L sublevels. Following the occurence of a K-level vacancy we have allowed one electron with energy $E_K - 2\bar{E}_L$ and two electrons with energies distributed uniformly in the interval $\bar{E}_L$ and $\bar{E}_L - E_F$ to appear. These rather crude approximations to the Auger spectra should be adequate here; it appears that the over-all slowing-down spectrum is rather insensitive to the details of these assumptions.

A vacancy in the conduction band whose energy lies below the maximum of the valence band by an amount in excess of g may be filled by an Auger process in which an electron appears in the conduction band. Auger electron-hole cascades in metals have been studied in the context of the electron-gas model.[30] In the present calculations we have ignored the contribution of valence-band-hole Auger processes to the slowing-down spectrum. We expect that at energies accessible in the experiment described above, such contributions will not be important.

B. Results of Calculations

The number of electrons generated in the slowing-down-cascade process increases quite markedly as the energy of a primary electron increases. To keep computing times small we decided to use the following approach. We assume that the slowing-down flux computed by the Spencer–Fano method is essentially correct for energies greater than $E_m = 10$ keV. Designating this flux by $\phi_{\text{SF}}(E)$, we compute numerically an equivalent source distribution $n(E)$ in the range of energies $E_g < E < E_m$ from the expression

$$n(E) = \sum_i \int_{E_m}^{\infty} dE' \left(\frac{d}{d\epsilon} \Sigma_{ip}(E, E') + \frac{d}{d\epsilon} \Sigma_{is}(E, E') + \frac{d}{d\epsilon} \Sigma_{iA}(E, E') \right). \quad (10)$$

Here $d\Sigma_{ip}(E, E')/d\epsilon$ represents the differential inverse mean free path for all processes in which electrons in the ith level (including those in the valence band) are excited by an energetic electron with energy E resulting in the degradation of this electron to the energy E', per unit energy interval. Similarly, $d\Sigma_{is}(E, E')/d\epsilon$ is the inverse mean free path for generation of a secondary electron with energy E' by a primary with energy E. The remaining inverse mean free path $d\Sigma_{iA}/d\epsilon$ is appro-

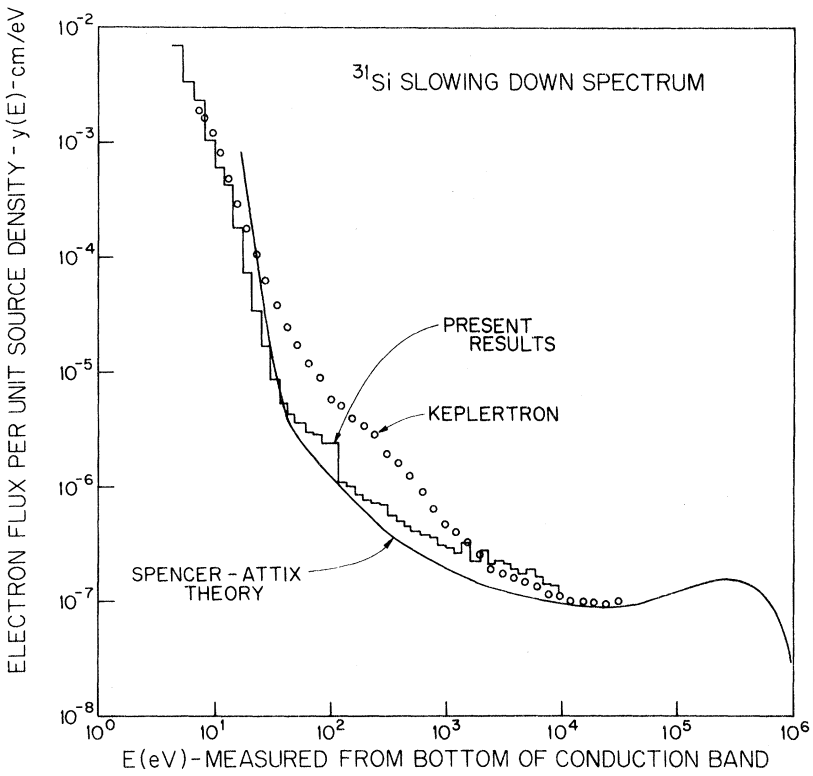

FIG. 10. Electron slowing-down spectrum in silicon. The points represent experimental data corrected to the interior of the sample. The smooth curve shows the results of calculations using the Spencer–Attix theory. The histogram gives results using the Monte Carlo approach described in the text.

priate to the generation of Auger electrons.

Adding to $n(E)$ the distribution $n_s(E)$, the number of electrons per unit volume per unit energy interval created directly from the uniformly distributed β source in the same interval, we arrive at an input source for our Monte Carlo slowing-down calculation. The cross sections described above are all derived from nonrelativistic theories; by contrast the Møller cross sections used by Spencer and Fano are fully relativistic and include exchange effects in the approximation that struck electrons are stationary and unbound. We allow for relativistic effects in an approximate way in evaluating the integrals appearing in Eq. (10). This correction involves simply replacing the inverse E multipliers of Eqs. (5) and (7) and the inverse ξ multiplier of Eq. (10) by their corresponding relativistically corrected forms. Although short of a complicated fully relativistic calculation which allows for exchange effects, this procedure should be adequate for the present purposes.

Figure 10 shows a comparison between (a) the experimental results for the slowing-down spectrum in Si, (b) the theoretical predictions using the Spencer–Attix theory, and (c) calculations using our model cross sections in a Monte Carlo program.[18,19] Calculations using the Spencer–Attix approach utilize the CSDA approximation to determine energy loss but treat the generation of secondary electrons using the Møller cross section.[31] The stopping power used in these calculations is computed from the Bethe formula except that stopping contributions from a given level are neglected for electron energies too low to excite that level.

The Monte Carlo results show a peaking at about 110 eV due to the presence of Auger electrons generated in the filling of holes in the L level. Auger electrons from K-level filling are not abundant enough to show up here. The Monte Carlo fluxes are generally smaller than the experimental fluxes except at the lowest energies considered. These differences are not well understood by us at present. It is possible that surface effects are responsible. Electrons with energies of the order of several keV may have ranges comparable with the thickness of oxidized or impurity layers at the surface. Such material might be subject to anomalous charging effects and might degrade electrons less efficiently than the bulk semiconductor material assumed in the theory. Efforts to understand the differences are continuing.

APPENDIX

We give explicit expressions for $\epsilon_1(k, \omega)$ and $\epsilon_2(k, \omega)$ on the basis of the Callaway–Tosatti[12,13] model.

In terms of the variables $\omega = \varkappa E_F/\hbar$ and $k = 2k_F z$, where $E_F \equiv \mathcal{R}(3\pi^2 a_0^3 n)^{2/3}$ and $k_F \equiv (3\pi^2 n)^{1/3}$, it is found that

$$\epsilon_2(k,\omega)=\frac{\pi\chi^2}{8z^3}\begin{cases} x-g, & g+4z(1-z)>x>g \\ \left[1-\left(z-\frac{x-g}{4z}\right)^2\right], & g+4z(1+z)>x>g+4z(1-z) \end{cases} \quad \text{(A1)}$$

where $g\equiv E_g/E_F$ and $\chi^2=(\mathcal{R}/\pi^2E_F)^{1/2}$. The Rydberg energy $\mathcal{R}=me^4/2\hbar^2=13.6$ eV. In addition, $\epsilon_2=0$ if $x<g$, if $x>g+4z(1+z)$, and if $x<g+4z(1-z)$. From the appropriate dispersion relations, it is found that[13]

$$\epsilon_1(k,\omega)=1+\frac{\chi^2}{z^2(8z+3g-gz^2)}\left\{4z+g+(g+x)\ln(g+x)+(g-x)\ln|g-x|\right.$$
$$+\left[1-\left(z+\frac{x+g}{4z}\right)^2\right]\ln|g+x+4z(1+z)|+\left[1-\left(z+\frac{g-x}{4z}\right)^2\right]\ln|g-x+4z(1+z)|$$
$$\left.-\left[1-\left(z-\frac{g+x}{4z}\right)^2\right]\ln|g+x+4z(1-z)|-\left[1-\left(z-\frac{g-x}{4z}\right)^2\right]\ln|g-x+4z(1-z)|\right\}, \quad \text{(A2)}$$

which is valid when $z<1$. In the case $z>1$,

$$\epsilon_1(k,\omega)=1+\frac{\chi^2}{z^2(8z+2g/z)}\left\{4z+\frac{g}{z}+\left[1-\left(z+\frac{g-x}{4z}\right)^2\right]\ln|g-x+4z(1+z)|\right.$$
$$+\left[1-\left(z+\frac{g+x}{4z}\right)^2\right]\ln|g+x+4z(1+z)|-\left[1-\left(z+\frac{g-x}{4z}\right)^2\right]\ln|g-x+4z(z-1)|$$
$$\left.-\left[1-\left(z+\frac{g+x}{4z}\right)^2\right]\ln|g+x+4z(z+1)|\right\}. \quad \text{(A3)}$$

It may be shown that for $z\to 0$,

$$\epsilon_1(k,\omega)=1+\frac{x_p^2}{g^2-x^2}, \quad \text{(A4)}$$

where $x_p=(\frac{16}{3}\chi^2)^{1/2}$ is the plasma resonance energy of the model semiconductor, measured in units of E_F. This form of ϵ_1 is quite plausible since it resembles the frequency-dependent dielectric permittivity of an assembly of classical electrons having binding energy gE_F.

*Research sponsored in part by the U. S. Atomic Energy Commission under contract with Union Carbide Corp. Research reported in this paper was supported in part by Defense Nuclear Agency through Air Force Cambridge Research Laboratories, Office of Aerospace Research, under Contract No. Y71-912, but the paper does not necessarily reflect endorsement by the sponsor.

[1]L. V. Spencer and U. Fano, Phys. Rev. 93, 1172 (1954). For detailed numerical evaluation of slowing-down fluxes for various materials using the Spencer–Fano theory, see R. M. McGinnies, NBS Circular No. 597, 1959 (unpublished).

[2]R. D. Birkhoff, in *Penetration of Charged Particles in Matter: A Symposium* (National Academy of Sciences, Washington, D.C., 1970), pp. 1–15.

[3]W. J. McConnell, H. H. Hubbell, Jr., R. N. Hamm, R. H. Ritchie, and R. D. Birkhoff, Phys. Rev. 138, A1377 (1965).

[4]J. H. Reynolds, Phys. Rev. 90, 1047 (1953).

[5]D. J. Hughes and R. B. Schwartz, Brookhaven National Laboratory Report No. BNL-325, July, 1958 (unpublished).

[6]W. S. Lyon and J. J. Manning, Phys. Rev. 93, 501 (1954).

[7]J. L. Blankenship (private communication).

[8]W. J. McConnell, R. D. Birkhoff, R. N. Hamm, and R. H. Ritchie, Radiat. Res. 33, 216 (1968).

[9]L. V. Spencer and F. H. Attix, Radiat. Res. 3, 239 (1955).

[10]C. E. Klots and H. A. Wright, Int. J. Radiat. Phys. Chem. 2, 191 (1970).

[11]C. H. Sherman and N. E. Gordon, Health Phys. 21, 733 (1971); Health Phys. 21, 743 (1971).

[12]J. Callaway, Phys. Rev. 116, 1368 (1959).

[13]E. Tosatti, Elementary Excitations in Anisotropic Semiconductors, Scuola Normale Superiore, Pisa, 1970 (unpublished). E. Tosatti and G. P. Parravicini, J. Phys. Chem. Solids 32, 623 (1971).

[14]For a review of work on this subject, see A. Burgess and I. C. Percival, in *Advances in Atomic and Molecular Physics* (Academic, New York, 1968), Vol. 4, p. 109. More recent research papers in this area are given in Refs. 8 and 9.

[15]J. D. Garcia, Phys. Rev. 177, 223 (1969).

[16]T. F. M. Bonsen and L. Vriens, Physica 47, 307 (1970).

[17]E. O. Kane, J. Phys. Soc. Japan Suppl. 21, 37 (1966); Phys. Rev. 159, 624 (1967).
[18]R. H. Ritchie, F. W. Garber, M. Y. Nakai, and R. D. Birkhoff, in *Advances in Radiation Biology*, edited by Leroy G. Augenstein, Ronald Mason, and Max Zelle (Academic, New York, 1969), Vol. III, pp. 1–28.
[19]R. H. Ritchie and V. E. Anderson, IEEE Trans. Nuclear Sci. NS-18, 141 (1971).
[20]For a recent review of this subject see *Studies in Penetration of Charged Particles in Matter*, NAS-NRC Publication No. 1133 (National Academy of Sciences, Washington, D. C., 1964).
[21]D. Penn, Phys. Rev. 128, 2093 (1962).
[22]W. Brandt and J. Reinheimer, Can. J. Phys. 46, 607 (1968).
[23]W. Brandt and J. Reinheimer, Phys. Letters 35, 109 (1971).
[24]L. Vriens and T. F. M. Bonsen, J. Phys. B 2, 1123 (1968).
[25]V. Fock, Z. Physik 98, 145 (1935).
[26]M. E. Rudd, D. Gregoire, and J. B. Crooks, Phys. Rev. A 3, 1635 (1971).
[27]U. Fano, Ann. Rev. Nucl. Sci. 13, 1 (1963).
[28]D. J. Bartelink, J. L. Moll, and N. I. Meyer, Phys. Rev. 130, 972 (1963).
[29]T. A. Carlson and M. O. Krause, Phys. Rev. 140, A1057 (1965).
[30]R. H. Ritchie, J. Appl. Phys. 37, 2276 (1966).
[31]The authors are indebted to R. N. Hamm for his work in numerically evaluating the Spencer–Attix equations in this connection.

PHYSICAL REVIEW B VOLUME 7, NUMBER 5 1 MARCH 1973

Paramagnetic Resonance and Relaxation of the Jahn–Teller Complex $[Ti(H_2O)_6]^{3+}$

N. Rumin, C. Vincent, and D. Walsh
Eaton Electronics Laboratory, McGill University, Montreal, Quebec, Canada
(Received 1 August 1972; revised manuscript received 1 November 1972)

The measured g values of the ground-state doublet of Ti^{3+} in methylammonium aluminum alum at 4.2 °K and below are shown to be incompatible with static crystal field theory. The measured spin-lattice relaxation rates in the range 1.45–2.85 °K can be described by either a two-Orbach process or a T^9 Raman process. A dynamic Jahn–Teller model due to Ham, which includes the interaction between an E_g vibrational mode and the $^2T_2$ electronic state, gives theoretical results which agree with both the measured g values and the two-Orbach relaxation process. Consequently, the agreement with the Raman process would appear to be fortuitous The measured g values and the two-Orbach process are described by $g_{\parallel}=1.37\pm0.01$, $g_{\perp}=1.61\pm0.01$, and $1/\tau=1.88\ e^{-14.52/T}+390.81\ e^{-27.41/T}\ \mu\text{sec}^{-1}$. The corresponding two excited doublets are at 10.5 ± 0.5 and 19.2 ± 2.0 cm^{-1}, respectively. Assuming a coupling to the E_g mode only, the deduced Jahn–Teller energy is 256 cm^{-1} and the effective mode frequency is 148 cm^{-1}. The ferroelectric transition from a structure with space group Pa3 to either space group $P2_1$ or $Pca2_1$ has a negligible effect on the EPR spectra, which in spite of the transition possess symmetry $(\bar{3})$.

I. INTRODUCTION

The crystal structure of methylammonium aluminum alum suggests that the Ti^{3+} ion is subjected to a predominantly cubic field with a small trigonal component. In a cubic field field of octahedral symmetry the free-ion ^2D ground state is split into a $^2T_2$ and an excited ^2E, which is 2×10^4 cm^{-1} or so above the ground state and may be neglected for our purposes. The octahedron is slightly flattened (Sec. II); consequently, using standard crystal field theory the combined spin-orbit and trigonal field splits the ground state into three Kramers doublets, the g values of the ground state doublet being given by

$$g_{\parallel}=2\left|\sin^2\theta-2\cos^2\theta\right|,$$
$$g_{\perp}=2\left|\sqrt{2}\sin\theta\cos\theta+\sin^2\theta\right|, \tag{1}$$

where

$$\sin2\theta=\frac{-\sqrt{2}\,\lambda}{[(V+\frac{1}{2}\lambda)^2+2\lambda^2]^{1/2}},$$

λ is the spin-orbit coupling, V is the trigonal splitting of the T_2 orbital state in the absence of spin-orbit coupling, and we have neglected covalency effects. The theory of Ti^{3+} in trigonal environments has received considerable attention,[1] and for all values of λ/V in Eq. (1), the inequality $g_{\parallel}\geq g_{\perp}$ holds. Our low-temperature paramagnetic-resonance spectra of Ti^{3+} in methylammonium minum alum, which is reported in Sec. III, gives for the ground doublet $g_{\perp}=1.61\pm0.01$ and $g_{\parallel}=1.37\pm0.01$, which is incompatible with static crystal field theory. The possibility that the trigonal field is reversed corresponding to a slightly elongated octahedron is untenable, since the resulting groundstate doublet is described by an effective